ANALYSIS OF THE FACTORS THAT INFLUENCE THE C=N STRETCHING FREQUENCY OF POLYENE SCHIFF BASES

Implications for Bacteriorhodopsin and Rhodopsin

HILLARY S. RODMAN GILSON,* BARRY H. HONIG,* ALAN CROTEAU,† GERARD ZARRILLI,† AND KOJI NAKANISHI†

Department of Biochemistry and Molecular Biophysics, Columbia University, 630 West 168th Street, New York, New York 10032; and †Department of Chemistry, Columbia University, New York, New York 10027

ABSTRACT In this study quantum mechanical calculations of force constants and normal mode analysis are used to elucidate the factors that influence the C=C and C=N stretching frequencies in polyenes and in protonated Schiff bases. The C=N stretching frequency is found to depend on both the C=N stretching force constant and the C=N—H bending force constant. Due to the contributions of these two modes, the C=N stretching frequency is particularly sensitive to the magnitude of the Schiff base counterion interactions and to the hydrogen bonding environment of the Schiff base nitrogen. Models for chromophore–protein interactions in the retinal binding site and for the photochemical transformations of bacteriorhodopsin and rhodopsin are evaluated in light of these results.

INTRODUCTION

Resonance Raman, infrared (IR), and Fourier transform infrared (FTIR) spectroscopy have been used extensively to study rhodopsin (the visual pigment in the rod cells of the retina), bacteriorhodopsin (the light-driven proton pump of *Halobacterium halobium*), and most recently, halorhodopsin (the light-driven chloride pump of *H. halobium*) (for a recent review see Mathies et al., 1987). Using these methods, the isomeric form and protonation state of the chromophore in these pigments have been determined. Information about chromophore–protein interactions may be obtained by comparing the spectroscopic properties of the pigments to those of the model compounds in solution, i.e., protonated and unprotonated retinal Schiff bases (SBs). Unfortunately, it is often difficult to interpret a change observed in a particular mode upon pigment formation in terms of a specific protein–chromophore interaction.

To aid in the interpretation of the vibrational data, it is in principle possible to develop force fields that accurately describe the molecules in question. Force fields are often determined empirically, by choosing force constants that reproduce measured frequencies. However, such force fields can be misleading since it is possible for different sets of force constants to yield similar frequencies. Furthermore, in the absence of a physical model for the factors that determine each force constant, even an accurate force field can provide only limited information. For example, if a particular force constant is different in a model compound and a pigment, a model for the source of the change cannot be derived without an understanding of the factors that determine the force constant. A normal mode analysis with an empirically determined force field provides no information in this regard. The problem can be solved, however, if force fields are calculated with quantum mechanical methods rather than from fitting procedures.

Unfortunately, quantum mechanical calculations are generally not sufficiently accurate to produce force fields that reproduce observed frequencies. However, it has been shown that by scaling the calculated force constants, very accurate force fields can be derived for small organic molecules (Pulay et al., 1983). Such a scaling is possible when errors in the calculations are systematic; for example, if all force constants for carbon–carbon stretches are overestimated by a constant percent. To the extent that this is the case, scaling will be superior to simple fitting procedures because the quantum mechanical calculations provide direct insights as to the underlying physical interactions that give rise to the force constants of the molecules.

In this study, scaled quantum mechanical force fields obtained from MINDO/3 calculations (Bingham et al., 1975) are used to elucidate the factors that determine the double bond stretching frequencies of retinal pigments and their model compound analogues. The primary concern is how $\nu_{C=N(H)}$ is influenced by changes in the environment of

the chromophore. An understanding of this question is needed to interpret the Raman and FTIR data of retinal containing pigments. In this regard, it is also important to understand how changes in the environment of the chromophore affect the C=C stretching modes.

METHODS

The MINDO/3 method was used to calculate the force constants because *ab initio* methods are not yet practical for the large molecules of interest in this study. (For an excellent review of semi-empirical methods see Sadlej, 1985.) Point charges were incorporated into this program by adding a Coulombic potential with a dielectric constant of 1 to account for the interaction of these charges with the molecule, i.e.,

$$E = \sum_{i}^{n} \frac{q_{pc}\ \rho_i}{R}, \qquad (1)$$

where ρ_i is the charge density of atom i, q_{pc} is the charge of the point charge, and R is the distance between them. Normal modes were obtained using the NORCOR program from QCPE.

The molecules were assumed to be planar (except for methyl groups). The molecular geometry was calculated by minimizing the molecular energy with respect to all the non-torsional degrees of freedom ($Q_1, \ldots Q_{2N-3}$), where N is the number of atoms in the molecule. The normal modes were calculated using this geometry. Complete force constant matrices $K_{ij} = \partial^2 E/\partial Q_i \partial Q_j$ were calculated for the polyenes ethylene, butadiene, and hexatriene. However, only the coupling constants shown in Table I were included for the model SB compounds (see Fig. 1) and octatetraene. These represent the minimum number of terms needed to reproduce the spectra of hexatriene. Including other coupling constants yielded negligible changes (<1 cm^{-1}) in the calculated frequencies.

The force constants and coupling constants were scaled to reproduce the spectra of butadiene. The same scaling factors were used for all polyenes. In SB and polyene Schiff bases (PSB) further scaling was applied to the force constants that involved the SB nitrogen (i.e., coordinates 7 [C=N], 31 [H16—C7—C6], and 32 [C=N—H]) to fit the frequencies of the molecule shown in Fig. 1 *b* (see Results). The coupling constants were originally scaled as

$$K_{ij}^{Sc} = S_i^{1/2} K_{ij} S_j^{1/2}, \qquad (2)$$

where K_{ij}^{Sc} is the scaled coupling constant, S_i and S_j are the scale factors for the diagonal force constants i and j, respectively, and K_{ij} is the

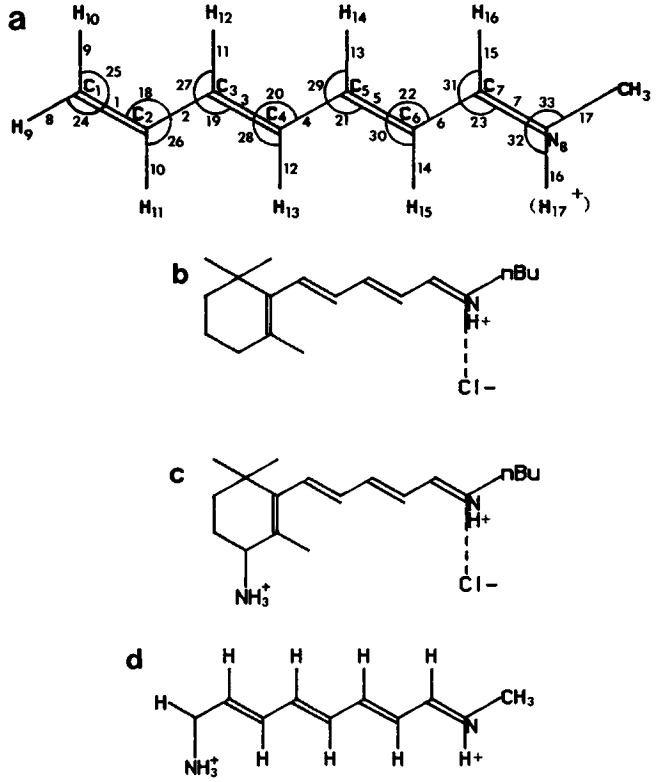

FIGURE 1 (*a*) Model Schiff base chromophore used in this study. Numbers indicate internal coordinates. (*b*) Frequencies for this retinal analogue with a Cl^- counterion in CH_2Cl_2 (Croteau, 1986) were used to scale the force constants for the C=N, C=N—H, and H16—C7—C6 coordinates. (*c*) One of the retinal analogues used by Sheves et al. (1986) to determine the effects of positive charges on the C=N stretching frequency (CH_2Cl_2 solvent with a Cl^- counterion). (*d*) Model compound used in this study to represent the chromophore shown in *c*, the counterion–nitrogen distance is 3.0 Å.

TABLE I
COUPLED INTERNAL COORDINATES MODES INCLUDED IN CALCULATIONS FOR THE MODEL SCHIFF BASES COMPOUNDS AND OCTATETRAENE

Coordinate	Coupled coordinates	Coordinate	Coupled coordinates
1	2–10, 18, 24–26	2	3–7, 10–11, 18–19, 26–27
3	4–7, 11–12, 19–20, 27–28	4	5–7, 12–13, 20–21, 28–29
5	6–7, 13–14, 21–22, 29–30	6	7, 14–15, 22–23, 30–31
7	15–17, 23, 31–33	8	9, 24–25
9	24–25	10	18, 26
11	19, 27	12	20, 28
13	21, 29	14	22, 30
15	23, 31	16	17, 32–33
17	32–33	18	26
19	27	20	28
21	29	22	30
23	31	32	33

Internal coordinates defined in Fig. 1.

TABLE II
COMPARISON BETWEEN CALCULATED AND OBSERVED FREQUENCIES OF BUTADIENE

Calc.	Obs.*	Calc.	Obs.	Calc.	Obs.
308	301	1,289	1,285 (1,296)	2,987	3,009 (3,014)
517	513	1,384	1,385	3,073	3,014
887	890	1,419	1,430 (1,442)	3,074	3,014 (3,056)
995	978 (991)	1,596	1,599	3,090	3,095 (3,101)
1,183	1,205	1,643	1,643	3,093	3,101 (3,102)
1,284	1,279 (1,291)	2,983	3,006 (2,985)		

*Observed values are taken from Gavin and Rice (1971), and Pulay et al. (1983) in parentheses.

calculated coupling constant (Pulay et al., 1983). If, however, the coupling constants are additionally scaled independently of the diagonal force constants, better agreement with observed frequencies is obtained. For this reason the coupling constants are first scaled as in Eq. 2 and then by an additional scale factor (see Results).

The λ_{max} for the model compounds are calculated using the PPP method parameterized for polyenes and protonated SBs using a dielectric constant of one (Honig et al., 1976).

RESULTS

Polyenes

Butadiene was used to scale the force constants since all the in-plane frequencies are known for this molecule. The scaling factors that gave the best agreement between observed and experimental frequencies are as follows: all stretching force constant were multiplied by 0.756, the CCC bending force constants were multiplied by 1.247, and the HCC bending force constants were multiplied by 1.172. In addition to the geometric scaling of the coupling constants (see Methods), the bend–bend interaction constants were reduced by a factor of 0.9, and the stretch–stretch interaction constants were increased by a factor of 1.5. The calculated frequencies are compared with observed frequencies in Table II. The 1,643-cm^{-1} band was used as the reference for the scaling. As is evident from Table II, excellent agreement between the calculated frequencies and observed frequencies is obtained. These results are comparable to those obtained with scaled *ab initio* force constants (Pulay et al., 1983). It should be noted that a good fit of the frequencies to butadiene can be obtained by using only a geometric scaling of the coupling constants. This scaling, however, does not transfer well to the larger polyenes. Including the additional scaling of the off-diagonal force constants results in excellent agreement between the calculated and observed frequencies for the series of polyenes ethylene to octatetraene (see below), thus demonstrating the transferability of these scaling parameters.

It is known that in linear polyenes there is a decrease in the highest frequency Raman active C=C stretching mode ($\nu_{C=C}$), as the length of the polyene increases. This behavior has been qualitatively explained in terms of an increase in π-electron delocalization as the length of the polyene increases; the decrease in $\nu_{C=C}$ being due to the fact that increased delocalization reduces the bond order of the double bonds and therefore their force constants. With one exception (Lasaga et al., 1980) previous studies have not reproduced this trend in the $\nu_{C=C}$ (Gavin and Rice, 1971; Warshel and Karplus, 1972). (See Kakitani et al., 1983 for a discussion of this problem.) Table III compares the calculated and experimental frequencies for the C=C stretching modes in ethylene, butadiene, hexatriene, and octatetraene. Excellent agreement with all the C=C stretching frequencies is obtained thus lending confidence in the reliability of the calculations.

SB and PSB

To simplify the calculations, the molecule shown in Fig. 1 *a* was used to represent the SB of retinal. The scaling used for polyenes was adopted for all bonds not involving the SB nitrogen. For the C=N stretch in the unprotonated SB the scaling factor of 0.756, used for C=C bonds in polyenes, yields $\nu_{C=N}$ = 1618. A small change in this value, using 0.771 instead of 0.756, gives the observed frequency of 1,630 (Croteau, 1986). The force constants of the protonated Schiff bases (PSBs) were scaled to fit the isotopic shifts observed in a series of model protonated retinal Schiff bases (PRSBs). (Croteau, 1986) (see Table IV), and to fit the frequencies of the molecule shown in Fig. 1 *b* (Croteau, 1986). Best results were obtained when the MINDO/3 value for $k_{C=N(H)}$ was multiplied by 0.816, $k_{C=N-H}$ by 1.141, $k_{H16-C7-C6}$ by 1.247, and the coupling between the C=N stretch and the C=N—H reduced by a factor of 0.4 (in addition to the scaling of Eq. 2). The force constants obtained for SB and PSB are given in Table V, and a comparison between observed and experimental frequencies for PSB in Table VI. The agreement over the

TABLE III
EXPERIMENTAL AND CALCULATED VALUES FOR THE RAMAN INTENSE $\nu_{C=C}$ IN CM^{-1}

	Ethylene*	Butadiene*		Hexatriene‡			Octatetraene‡			
Exp.	R 1,630	R 1,643	1,599	1,623	R 1,623	R 1,573	1,631	R 1,612	R 1,608	NA
Calc.	1,631	1,643	1,598	1,624	1,621	1,582	1,625	1,616	1,598	1,573

Raman active mode is denoted by R. NA, not available.
*Gavin and Rice (1971).
‡Observed values taken from Hudson et al. (1982).

TABLE IV
ISOTOPIC SHIFTS IN PRSB

	N–D	^{15}N	CD	CD, ^{15}N	^{13}C	$^{13}C^{15}N$	^{13}CD	^{13}CD ^{15}N
Exp.*	19–24	11–15	7–15	24–29	17–22	31–33	26–32	40–55
Calc.	22	21	11	33	24	44	33	54

Range of values given include PRSB in methanol, and PRSB in CH_2Cl_2 with chloride, trifluroacetate, and BF_4 counterions. C stands for carbon 15, CD stands for a deuterium substitution on carbon 15. The calculated values are the results from using the model compound shown in Fig. 1 *a*.
*Experimental values from Croteau (1986).

full range of frequencies is quite good, demonstrating the transferability of the polyene force field to SBs. (Note that only a few frequencies are affected by the additional scaling of C=N-related bonds.) It should be noted that the calculated ^{13}C and ^{15}N shifts are larger than those observed experimentally. This discrepancy could result from a lesser degree of mixing in the model compounds, which are smaller than PRSB and thus have less extended modes.

The preceding analysis predicts a k_{C-N} for the SB that is slightly larger but quite close to that of the PSB. This appears surprising given that the λ_{max} of PSBs are higher and ν_{C-C} are lower than those in SBs. Both these facts indicate that there is greater π-electron delocalization in PSBs than SBs and thus suggest that the force constant of the C=N stretch in PSBs ($k_{C-N(H)}$) should be considerably larger than the force constant of SBs (k_{C-N}). However, Lopez-Garriga et al. (1986*a*, *b*) have argued that the σ-electron density from the lone pair on the nitrogen moves into the C=N bond upon protonation and increases $k_{C-N(H)}$ relative to k_{C-N}. Given the uncertainties inherent both in the quantum mechanical calculations and in the scaling, the force constants we obtain are not accurate enough to be used as a basis for arguing which force constant is larger. In either case, it is clear from our analysis that the high value of $\nu_{C-N(H)}$ in protonated Schiff bases is caused by an interaction of the C=N stretch with the C=N—H bend in agreement with the original suggestion of Aton et al. (1980). (In deuterated Schiff bases, the C=N stretching mode has much smaller contributions from the C=N—D bend.) The crucial importance of the C=N—H bend in determining the C=N stretching frequency is consistent with a recent experimental study of Baasov et al. (1987).

νC=N(H)

Fig. 3 and Table VII show the correlation of $\nu_{C-N(H)}$ with changes in λ_{max}, where the λ_{max} is varied either by changing the counterion distance or by placing point charges around the chromophore, and keeping the counterion at 3.0 Å. The only compound for which there are experimental data is that labeled C1+. The compound used in the experiment contains a positive charge on the β-ionone ring, as shown in Fig. 1 *c*. (The model used to represent this compound in the calculations is shown in Fig. 1 *d*.) The positive charge was found to shift $\nu_{C-N(H)}$ by only 4 cm^{-1}, even though the λ_{max} shifts by 4,600 cm^{-1} (Baasov et al., 1987). Our calculations are in good agreement with these data showing a shift in λ_{max} of 3,900 cm^{-1} and a change in $\nu_{C-N(H)}$ of only 6 cm^{-1}.

The main point illustrated in Fig. 2 is that $\nu_{C-N(H)}$ is much more sensitive to changes in the SB–counterion interaction than to changes elsewhere in the molecule. This is because the counterion distance affects both k_{C-N-H} and $k_{C-N(H)}$, while k_{C-N-H} is not very sensitive to changes induced elsewhere in the molecule. For example, moving the counterion from 2.75 Å to ∞ causes a shift in λ_{max} of 3,850 cm^{-1} and a decrease in $\nu_{C-N(H)}$ of 106 cm^{-1}. In contrast, the difference in λ_{max} between placing a negative charge near C7 and placing a negative charge near C1 is 9,050 cm^{-1}, but $\nu_{C-N(H)}$ shifts by only 39 cm^{-1}. It thus appears that there is a high correlation between λ_{max} and $\nu_{C-N(H)}$ for chromophores differing only in the counterion distance, and a weaker correlation between λ_{max} and $\nu_{C-N(H)}$ for molecules varying only in the location of the second charge (see also Discussion). The latter correlation disappears completely for the molecules that absorb at longer wavelengths than PSB (see Fig. 2).

In separate calculations, we find essentially no effect on the deuterium shift when charges are placed around the chromophore, since these perturbations do not affect k_{C-N-H}. Thus, the results of this section suggest that a decrease in $\nu_{C-N(H)}$ and a reduced deuteration shift in a particular pigment relative to a model compound (or to another pigment) are strong indications for the presence of a weaker SB–counterion interaction.

νC=C

A plot of the three ν_{C-C} versus λ_{max} for the PSB molecules with counterion distances ranging form 2.75 Å to ∞ is shown in Fig. 3. The top line marked with triangles is primarily the C1=C2 stretching mode the second line is primarily C3=C4 (*squares*); and the bottom mode is primarily C5=C6 (*circles*). All three frequencies are strongly correlated with λ_{max}. It is the middle mode that corresponds to the observed Raman intense C=C stretching mode. Both the frequency of this mode and its correlation with λ_{max} agree well with experimental data (Aton et al., 1977). (The slope of the middle plot is −0.288 with a *y* intercept of 1,681, compared with the observed slope of −0.243 and *y* intercept of 1,666). The C5=C6 stretching mode shows a stronger response to moving the counterion away then the other two C=C stretching modes.

DISCUSSION

Implications for bR

As can be seen in Table VIII, bR_{568} has a smaller $\nu_{C-N(H)}$ and deuteration shift in $\nu_{C-N(H)}$ than does PRSB. As discussed above, the smaller deuteration effect is good evidence that the reduced $\nu_{C-N(H)}$ is due to a weaker

TABLE V
SCALED FORCE CONSTANTS FOR SB AND RSB

Diagonal force constants

IC	PSB	SB	IC	PSB	SB	IC	PSB	SB
1	9.068	9.097	12	5.006	4.910	23	1.564	1.484
2	5.518	5.527	13	4.867	4.907	24	0.929	0.935
3	8.448	8.570	14	5.034	4.918	25	0.929	0.928
4	5.532	5.521	15	4.796	4.222	26	1.107	1.122
5	8.253	8.565	16	4.048		27	1.161	1.149
6	5.409	5.360	17	5.301	5.312	28	1.124	1.151
7	10.175	10.258	18	1.236	1.244	29	1.182	1.159
8	5.258	5.239	19	1.328	1.321	30	1.142	1.170
9	5.220	5.216	20	1.343	1.346	31	1.295	1.226
10	4.982	4.928	21	1.344	1.335	32	1.296	
11	4.896	4.908	22	1.403	1.371	33	1.065	0.521

Coupling constants

Stretch–stretch couplings

CC	PSB	SB	CC	PSB	SB	CC	PSB	SB
1-2	0.947	0.916	2-7	0.022	0.006	4-13	0.328	0.320
1-3	−0.058	−0.041	2-10	0.312	0.320	5-6	1.159	0.878
1-4	0.067	0.043	2-11	0.319	0.318	5-7	−0.181	−0.037
1-5	−0.027	−0.013	3-4	1.057	0.947	5-13	0.393	0.400
1-6	0.021	0.005	3-5	−0.115	−0.052	5-14	0.371	0.400
1-7	−0.012	−0.002	3-6	0.122	0.040	6-7	1.303	1.062
1-8	0.365	0.380	3-7	−0.061	−0.012	6-14	0.320	0.309
1-9	0.378	0.386	3-11	0.392	0.401	6-15	0.279	0.330
1-10	0.402	0.404	3-12	0.397	0.403	7-15	0.524	0.873
2-3	0.921	0.908	4-5	1.019	0.947	7-16	0.565	
2-4	−0.036	−0.008	4-6	−0.113	−0.006	7-17	1.020	0.822
2-5	0.060	0.042	4-7	0.103	0.043	8-9	0.156	0.159
2-6	−0.031	−0.006	4-12	0.306	0.318	16-17	0.376	

Stretch–bend couplings

CC	PSB	SB	CC	PSB	SB	CC	PSB	SB
1-18	0.097	0.091	5-21	0.090	0.103	10-18	−0.287	−0.297
1-24	0.308	0.313	5-22	0.437	0.432	10-26	−0.019	−0.022
1-25	0.295	0.297	5-29	−0.311	−0.317	11-19	−0.298	−0.295
1-26	−0.308	−0.306	5-30	0.304	0.321	11-27	−0.022	−0.018
2-18	0.405	0.401	6-22	0.065	0.071	12-20	−0.263	−0.277
2-19	0.405	0.412	6-23	0.449	0.468	12-28	0.013	0.018
2-26	0.311	0.300	6-30	−0.381	−0.322	13-21	−0.302	−0.292
2-27	0.288	0.297	6-31	0.247	0.308	13-29	−0.025	−0.015
3-19	0.094	0.103	7-23	0.086	0.057	14-22	−0.239	−0.270
3-20	0.446	0.433	7-31	−0.352	−0.373	14-30	−0.015	0.022
3-27	−0.312	−0.315	7-32	0.163		15-23	−0.304	−0.286
3-28	0.319	0.317	7-33	0.487	0.786	15-31	−0.052	0.012
4-20	0.091	0.099	8-24	0.038	0.038	16-32	−0.040	
4-21	0.404	0.415	8-25	−0.206	−0.212	16-33	−0.216	
4-28	−0.327	−0.305	9-24	−0.208	−0.211	17-32	−0.318	
4-29	0.285	0.301	9-25	0.040	0.037	17-33	0.098	0.647

Bend-bend Couplings

CC	PSB	SB	CC	PSB	SB	CC	PSB	SB
18-26	0.493	0.501	21-29	0.551	0.530	24-25	0.409	0.410
19-27	0.536	0.526	22-30	0.591	0.562	32-33	0.474	
20-28	0.538	0.545	23-31	0.709	0.615			

See Fig. 1 *a* for numbering of internal coordinates (IC). CC stands for coupled coordinates.

TABLE VI
COMPARISON OF OBSERVED IR FREQUENCIES OF THE MOLECULE SHOWN IN FIG. 1 *b*, AND THE CALCULATED FREQUENCIES

Obs.*	Calc.	Description
	2,694	N—H
1,665	1,665	C=N and C=N—H
1,598	1,598	C1=C2
1,576	1,564	C3=C4
1,528	1,507	C5=C6
1,445	1,445	C=N—H bend
1,421	1,421	HCC bend
1,376	1,381	
1,365	1,349	
1,345	1,327	
1,303	1,300	
1,276	1,271	
1,169	1,166	C2—C3, C6—C7 and C4—C5
1,143	1,149	C4—C5 and C2—C3
1,117	1,118	C6—C7 and C4—C5

The description indicates the major component of the mode.
*Croteau (1986).

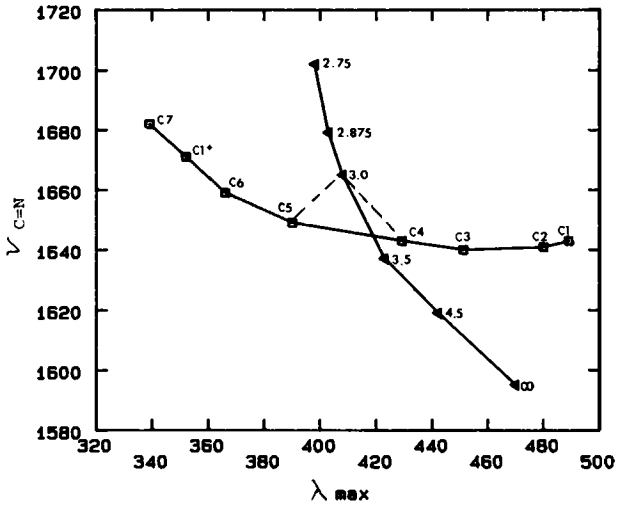

FIGURE 2 Plot of λ_{max} versus the C=N stretching frequency, for molecules differing in counterion distance only (labeled with the counterion distance), and with the same counterion distance, but different locations of a second charge. See Table VII for the definition of the labels.

counterion interaction. The most recent studies on the protein–chromophore interactions in bR (Harbison et al., 1985; Spudich et al., 1986; Gilson and Honig, 1988) based on solid state NMR and absorption spectroscopy, indicate that there is a charge pair by the ring, and a "weak" counterion (relative to PRSB with a chloride counterion) in bR. It should be noted that there is an aspartate residue (asp-212) one turn of the helix away from the SB nitrogen in the sequence of bR (Khorana et al., 1979; Ovchinnikov et al., 1979). This residue is likely to be the SB counterion.

Upon absorbing light, the retinal chromophore of bR isomerizes from all-*trans* to 13-*cis*. The resulting photoproduct, K_{625}, has an increased λ_{max}, and a decreased $\nu_{C-N(H)}$ (Mathies et al., 1987). As has been pointed out (Honig et al., 1979), the spectroscopic red-shift and increase in energy that accompanies the primary event can be explained if the isomerization causes the SB proton to break its salt bridge with, and move away from, its counterion. Interpreted in its simplest form, this model implies that the SB in bR forms a hydrogen bond to its salt bridge partner, whereas the hydrogen bond is completely

TABLE VII
THE CALCULATED λ_{max} (in nm), $\nu_{C-N(H)}$, ν_{C-C} (C3=C4), AND DEUTERATION SHIFTS IN $\nu_{C-N(H)}$ ($\Delta\nu_{deu}$) (in cm^{-1}) FOR THE MODEL CHROMOPHORES USED IN THIS STUDY

Molecule	λ_{max}	$\nu_{C-N(H)}$	ν_{C-C}	$\Delta\nu_{deu}$
2.75	398	1,702	1,567	45
2.875	403	1,679	1,565	29
3.0	408	1,665	1,564	22
3.5	423	1,640	1,560	13
4.5	442	1,621	1,554	10
NCA	470	1,595	1,531	8
C7	339	1,682	1,570	19
C6	366	1,659	1,570	22
C5	390	1,649	1,568	22
C4	429	1,643	1,564	23
C3	451	1,640	1,555	23
C2	480	1,641	1,550	24
C1	489	1,643	1,545	23
C+	352	1,671	1,555	23

The PSBs without a second ion are identified by their counterion distance (NCA denotes PSB without a counterion). The molecules labeled with atom numbers indicate PSB molecules with second ions located 3.0 Å from the atom in the label and above the plane of the chromophore. All molecules with second ions have a counterion distance (CA) of 3.0 Å. The molecule C+ is shown in Fig. 1 *d*.

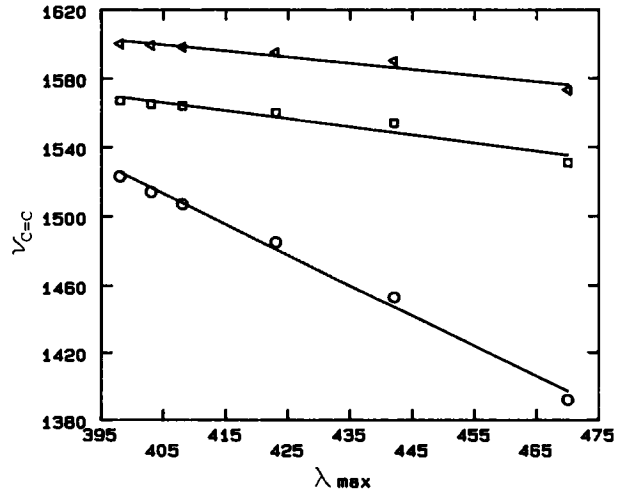

FIGURE 3 Plot of λ_{max} versus frequency for the C1=C2 (*triangles*), C3=C4 (*squares*), and C5=C6 (*circles*) stretching modes of molecules with counterion distances between 2.75 and 4.5 Å and with no counterion.

TABLE VIII
SPECTRAL PROPERTIES OF RETINAL CONTAINING PIGMENTS AND THEIR PHOTOPRODUCTS

	$\nu_{C-N(H)}$	$\nu_{C-N(D)}$	$\Delta\nu_{deu}$	ν_{C-C}
$PRSB_{444}$ (MeOH)*	1,656	1,632	24	1,557
Bacteriorhodopsin				
bR_{568}‡	1,642	1,624	18	1,530
K_{625}‡	≤1,620			1,514
Rhodopsin				
$Rhod_{498}$§	1,660	1,629	31	1,545
$Batho_{543}$§	1,657	1,625	32	1,536

λ_{max} is subscripted (in nm); $\nu_{C-N(H)}$, ν_{C-C}, $\Delta\nu_{deu}$, and $\nu_{C-N(D)}$ in cm^{-1}.
*Croteau (1986).
‡Stockburger et al. (1982).
§Mathies et al. (1987).

broken in K. The present analysis clearly indicates that the absence of a hydrogen bond should cause K to have a lower $\nu_{C-N(H)}$ than bR. That this is observed experimentally is thus consistent with the predictions of the charge separation model, as has been pointed out previously (Rothschild and Marrero, 1982). However, the data don't really distinguish between the absence of a hydrogen bond and the possibility of a weaker hydrogen bond in K than in bR.

It is interesting to note that ν_{C-N-H} has been assigned to 1,350 cm^{-1} in bR (Massig et al., 1982). We have found (Gilson, H. S. R., and B. H. Honig, unpublished results) that in molecules where there is a weak SB–counterion interaction, the C=N—H bending mode delocalizes, and a mode around 1,350 cm^{-1} is predicted to gain C=N—H bending character (see Results). The calculations also indicate that the primary C=N—H bending mode should be around 1,400 cm^{-1}, as suggested by Lopez-Garriga et al. (1986*a*). However, intensity calculations (using the method described in Kakitani et al., 1983) indicate that this mode loses Raman intensity as the counterion–SB interaction decreases. Consequently, this peak may have very little Raman intensity and may not be detectable in most pigments.

Implications for Rhodopsin

Rhodopsin has a $\nu_{C-N(H)}$ of about 1,660 cm^{-1} and an unusually large deuterium shift of ~30 cm^{-1}. Although $\nu_{C-N(H)}$ is similar to that of model protonated SBs, the large deuterium shift suggests that the SB nitrogen in rhodopsin interacts strongly with a hydrogen bonding group. It has been commonly assumed that this group corresponds to a carboxylate counterion. However, in contrast to bR, where asp-212 is an obvious choice for the counterion (see above), there is no negatively charged residue in the primary sequence of rhodopsin which is close to the retinal chromophore (Ovchinnikov et al., 1982; Hargrave et al., 1983). There are other candidates in the rhodopsin sequence but the possibility must be considered that there is no negatively charged counterion and that the SB proton interacts with one or more dipolar groups in the protein that provide hydrogen bonding and electrostatic stabilization equivalent to that provided by a negatively charged counterion. As an example supporting this possibility, the absorption maximum of PRSB in methanol is bluer than in nonpolar solvents, and both $\nu_{C-N(H)}$ and the deuterium shift are larger in methanol (Croteau, 1986). These observations indicate that the electrically neutral dipoles of methanol can interact more strongly with the SB than can a single negative charge.

Another way the protein could provide electrostatic stabilization of the SB is through the use of α-helix dipoles. There are numerous examples where helix dipoles stabilize charge groups in globular proteins (Hol, 1985). Their effect, however, is largest near the helix termini. While most models of rhodopsin based on sequence analysis place the retinal near the middle of a helix, Findlay (1986) has pointed out that the existence of prolines in the putative rhodopsin helices might disrupt their regular structure for a few turns. The existence in all known visual pigments (Findlay, 1986; Applebury and Hargrave, 1986) of a conserved proline seven residues away from the lysine containing the retinal and a conserved asparagine (also a strong helix breaker) adjacent to the proline suggest that the helix containing the retinal may indeed be disrupted. A break in the helix could produce large electric fields in the vicinity of the SB which could provide a stabilizing interaction with the chromophore.

The primary photochemical event in rhodopsin is an 11-*cis* → all-*trans* isomerization of the retinal chromophore. The isomerization, which results in the formation of bathorhodopsin, is accompanied by a spectroscopic red-shift (to 543 nm) and a large enthalpy increase (35 kcal/mol; Cooper, 1979). The isomerization–charge separation model (Honig et al., 1979) accounts for these observations as it does for the primary photochemical event in bR. However, in contrast to bR (see above), the model appears to be inconsistent with the fact that both $\nu_{C-N(H)}$ and the deuteration shift remain essentially unchanged in bathorhodopsin. Indeed the large deuteration shift in bathorhodopsin clearly indicates that its Schiff base is strongly hydrogen bonded. Thus, the charge separation model, interpreted as for bR to imply the breaking of a salt bridge and the displacement of the SB to a location where it forms no (or very weak) hydrogen bonds, cannot be correct for the rhodopsin–bathorhodopsin transformation.

It is possible, however, to conceive of models in which the strengths of the hydrogen bonds in rhodopsin and bathorhodopsin are similar but where the electric field near the SB changes during the course of the isomerization. This might occur, for example, if the SB moved away from its counterion but interacted with one or more neutral hydrogen bonding groups in bathorhodopsin. Alternatively, if there is no direct counterion in rhodopsin (see above), electrostatic energy storage might be achieved if the SB were displaced in an electric field produced by other

structural elements of the protein such as the dipole moment of an α-helix. While these suggestions are of course purely speculative, they do offer the possibility of retaining the attractive features of the charge-separation model while remaining consistent with the vibrational analysis. Another possibility is offered by the suggestion of Birge and co-workers (1985) that the counterion is located below the C=N bond but does not directly hydrogen bond to the nitrogen. In this case, the hydrogen bond required by the Raman data could be provided by a group on the protein or by a bound water.

If models such as those mentioned in the previous paragraph are to be entertained, it is important to estimate the expected shift in $\nu_{C-N(H)}$ when the electrostatic potential near the SB is changed while the hydrogen bonding remains constant (if for example one hydrogen bond is broken and a new one is formed during the rhodopsin–bathorhodopsin transformation). Baasov and Sheves (1985) have synthesized a series of iminium salts of PRSB analogues (the SB in this case cannot form a hydrogen bond) and then studied the effects of the addition of charged substituents on these compounds. They found that positive substituents located as close as 2 Å from the Schiff base shifted λ_{max} by ~30 nm (490–520 nm) and ν_{C-C} by 14 cm^{-1}, while inducing only small (3–6 cm^{-1}) shifts in ν_{C-N}. Charges located somewhat further from the SB, while affecting λ_{max} and ν_{C-C}, had essentially no effect on ν_{C-N}. These considerations appear to allow for a model in which the electrical potential near the SB is different in rhodopsin and bathorhodopsin as long as both species contain strong hydrogen bonds.

In summary, we have shown that semi-empirical calculations of force constants when combined with normal mode analysis can enhance our ability to interpret Raman and IR measurements. We have succeeded in accounting for the relationship between ν_{C-C} and chain length in linear polyenes, and applied the force field so derived to SBs and protonated SBs. Our analysis of these molecules is consistent with the studies of Sheves and co-workers (Baasov and Sheves, 1985; Baasov et al., 1987) on related model compounds and, taken together, provide an understanding of the factors that determine the vibrational spectra of retinal analogues and retinal pigments. Having a reliable theoretical framework for interpreting these spectra in terms of specific physical interactions (i.e., the effect of external charges) provides a firm basis for the evaluation of models that account for the function of retinal pigments.

We wish to thank Robert Callender, Michael Gilson, and Philippe Youkharibache for many helpful discussions.

This work was supported by National Science Foundation (DMB85-03489) and National Institutes of Health (GM30518) and (GM36564).

Received for publication 20 July 1987 and in final form 6 October 1987.

REFERENCES

Applebury, M. L., and P. A. Hargrave. 1986. Molecular biology of visual pigments. *Vision Res.* 26:1881–1895.

Aton, B., A. G. Doukas, R. H. Callender, B. Becher, and T. G. Ebrey. 1977. Resonance Raman studies of the purple membrane. *Biochemistry.* 16:2995–2999.

Aton, B., A. G. Doukas, D. Navra, R. H. Callender, U. Dinur, and B. Honig. 1980. Resonance Raman studies of the primary photochemical event in visual pigments. *Biophys. J.* 29:70–94.

Baasov, T., and M. Sheves. 1985. Model compounds for the spectroscopic properties of visual pigment and bacteriorhodopsin. *J. Am. Chem. Soc.* 108:7524–7533.

Baasov, N. Friedman, and M. Sheves. 1987. Factors affecting the C=N stretching frequency of protonated retinal Schiff bases. A model study for bacteriorhodopsin and visual pigments. *Biochemistry.* 26:3210–3217.

Bingham, R. C., M. J. S. Dewar, and D. H. Lo. 1975. Ground states of molecules. XXV. MINDO/3. An improved version of the MINDO semiempirical SCF-MO method. *J. Am. Chem. Soc.* 97:1285–1293.

Birge, R., C. Einterz, H. Knapp, and L. Murray. 1988. The nature of the primary photochemical events in rhodopsin and isorhodopsin. *Biophys. J.* In press.

Cooper, A. 1979. Energy uptake in the first step of visual excitation. *Nature (Lond.).* 282:531–533.

Croteau, A. 1986. Spectroscopic and synthetic studies of retinal rhodopsin and bacteriorhodopsin analogs. Ph.D. Thesis, Columbia University, New York.

Findlay, J. B. C. 1986. The Molecular Mechanism of Photoreception. H. Stieve, editor. Dahlem Konferenzen 1986, Springer-Verlag, Berlin, Heidelberg, New York, Tokyo. 11–30.

Gavin, R. M., and S. A. Rice. 1971. Correlation of pi-electron density with vibrational frequencies of linear polyenes. *J. Chem. Phys.* 55:2675–2681.

Gilson, H. S. R., and B. H. Honig. 1988. Analysis of NMR and absorption spectroscopic data in bacteriorhodopsin: models for protein-chromophore interactions. *J. Am. Chem. Soc.* In press.

Harbison, G. S., S. O. Smith, J. A. Pardoen, J. M. L. Courtin, J. Lugtenburg, J. Herzfeld, R. A. Mathies, and R. G. Griffin. 1985. Solid-state ^{13}C NMR detection of a perturbed 6-s-trans chromophore in bacteriorhodopsin. *Biochemistry.* 24:6955–6962.

Hargrave, P. A., J. J. McDowell, D. R. Curtis, J. K. Wang, E. Juszczak, S.-L. Fong, J. K. M. Rao, and P. Argos. 1983. The structure of bovine rhodopsin. *Biophys. Struct. Mech.* 9:235.

Hol, W. G. J. 1985. The role of the α-helix dipole in protein function and structure. *Prog. Biophys. Mol. Biol.* 45:145–195.

Honig, B., A. Greenberg, U. Dinur, and T. G. Ebrey. 1976. Visual-pigment spectra: implications of the protonation of the retinal Schiff base. *Biochemistry.* 15:4593–4599.

Honig, B., T. Ebrey, R. H. Callender, U. Dinur, and M. Ottolenghi. 1979. Photoisomerization, energy storage, and charge separation: a model for light energy transduction in visual pigments and bacteriorhodopsin. *Proc. Natl. Acad. Sci. USA.* 76:2503–2507.

Hudson, B. S., B. E. Kohler, and K. Schulten. 1982. Linear polyene electronic structure and potential surfaces. *Excited States.* 6:1–95.

Kakitani, K., T. Kakitani, H. Rodman, B. Honig, and R. Callender. 1983. Correlation of vibrational frequencies with absorption maxima in polyenes, rhodopsin bacteriorhodopsin, and retinal analogues. *J. Phys. Chem.* 87:3620–3628.

Khorana, H. G., G. E. Gerber, W. C. Herlihy, C. P. Gray, R. J. Anderegg, K. Nihei, and K. Biemann. 1979. Amino acid sequence of bacteriorhodopsin. *Proc. Natl. Acad. Sci. USA.* 76:5046–5050.

Lasaga, A. C., R. J. Aerni, and M. Karplus. 1980. Photodynamics of polyenes: the effect of electron correlation on potential surfaces. *J. Chem. Phys.* 73:5230–5242.

Lopez-Garriga, J. J., G. T. Babcock, and J. F. Harrison. 1986*a*. Factors influencing the C=N stretching frequency in neutral and protonated Schiff's bases. *J. Am. Chem. Soc.* 108:7241–7251.

Lopez-Garriga, J. J., S. Hanton, G. T. Babcock, J. F. Harrison. 1986*b*. Rehybridization of the C=N bond upon protonation of methylimine increases the C=N stretching force constant. *J. Am. Chem. Soc.* 108:7251–7254.

Massig, G., M. Stockburger, W. Gartner, D. Oesterhelt, and P. Towner. 1982. Structural conclusion on the Schiff base group of retinylidene chromophores in bacteriorhodopsin from characteristic vibrational bands in the resonance raman spectra of bR_{570} (all-trans), bR_{603} (3-dehydroretinal and bR_{548} (13-cis). *J. Raman Spectrosc.* 12:287–294.

Mathies, R. A., S. O. Smith, and I. Palings. 1987. Determination of retinal chromophore structure in rhodopsins. *In* Biological Applications of Raman Spectroscopy. T. G. Spiro, editor. John Wiley & Sons, New York. vol. 2, pp. 59–109.

Ovchinnikov, Y. A., N. G. Abdulaev, M. Y. Feigina, A. V. Kiselev, and N. A. Lobanov. 1979. The structural basis of the functioning of bacteriorhodopsin: an overview. *FEBS (Fed. Eur. Biochem. Soc.) Lett.* 100:219–224.

Ovchinnikov, Y. A., N. G. Abdulaev, M. Y. Feigina, I. D. Artamonov, A. S. Zolotarev, M. B. Kostina, A. S. Bogachuk, A. I. Miroshnikov, V. I. Martinov, and A. B. Kudelin. 1982. The complete amino acid sequence of visual rhodopsin. *Bioorg. Khim.* 8:1011–1014.

Pulay, P., G. Fogarasi, G. Pongor, J. E. Boggs, and A. Vargha. 1983. Combination of theoretical ab initio and experimental information to obtain reliable harmonic force constants. Scaled quantum mechanical (SQM) force fields for glyoxal, acrolein, butadiene, formaldehyde, and ethylene. *J. Am. Chem. Soc.* 105:7037–7047.

Rothschild, K. J., and H. Marrero. 1982. Infrared evidence that the Schiff base of bacteriorhodopsin is protonated: bR570 and K intermediates. *Proc. Natl. Acad. Sci. USA.* 79:4045–4049.

Sadlej, J. 1985. Semi-Empirical Methods of Quantum Chemistry. Halsted Press Limited, West Sussex.

Spudich, J. L., D. A. McCain, K. Nakanishi, M. Okabe, N. Shimizu, H. Rodman, B. Honig, and R. A. Bogomolni. 1986. Chromophore/protein interaction in bacterial sensory rhodopsin and bacteriorhodopsin. *Biophys. J.* 49:479–483.

Stockburger, M., W. Klusmann, H. Gattermann, and G. Massig. 1979. Photochemical cycle of bacteriorhodopsin studied by resonance Raman spectroscopy. *Biochemistry.* 18:4886–4892.

Warshel, A., and M. Karplus. 1972. Calculation of ground and excited state potential surfaces of conjugated molecules. I. Formulation and parameterization. *J. Am. Chem. Soc.* 94:5612–5625.